DEJA HUELLA EN EL ICMUV

CUARTAS JORNADAS JÓVENES ICMUV

Viernes, 21 junio 2019, 12:30h

ICMUV
INSTITUT DE CIÈNCIA DELS MATERIALS de la Universitat de València

CUARTAS JORNADAS JÓVENES ICMUV

1

- **Caracterización estadística de ruido de emisión espontánea amplificada de banda angosta**
  Pablo Muniz-Cánovas, Yuri Barmenkov, Alexander Kir'yano, José L. Cruz, Miguel Andrés

2

- **Polarization Modulation Instability in all-normal Dispersion Microstructured Optical Fibers**
  A. Loredo-Trejo, Y. López-Dieguez, A. Díez, E. Silvestre and M. V. Andrés

3

- **Refining two-dimensional semiconductors photoluminescence emission: SiO2 microspherical resonators in WSe2 and InSe**
  Daniel Andres-Penares, Juan P. Martínez-Pastor, Carlos J. Zapata-Rodriguez and Juan F. Sánchez-Royo

4

- **All-polarization-maintaining mode-locked thulium-doped fiber laser**
  L.A. Sánchez, A. Carrascosa, L. Escalante-Zárate, J.L. Cruz, A. Díez, and M.V. Andrés

5

- **High-pressure characterization of the optical and electronic properties of InVO4, InNbO4, and InTaO4**
  P. Botella, D. Errandonea, A. B. Garg, P. Rodriguez-Hernandez, A. Muñoz, S. N. Achary, A. Vomiero

6

- **Printed luminescent chemosensor for detection of nitroderivate compounds**
  Eduardo Aznar, Rafael Abargues, Juan P. Martínez-Pastor, Pedro Rodríguez-Cantó

7

- **Multi-analytical characterization of Valencian artists' palette from the XIX-XX centuries.**
  Silvia Caravá, Francesca C. Izzo, Clodoaldo Roldán García, María Luisa Vázquez de Agredos Pascual, Sonia Murcia Mascarós

8

- **Characterization of optical fibers photosensitivity by means of in-fiber acousto-optic interaction**
  Saúl Rosales-Mendoza, Martina Delgado-Pinar, José Luis Cruz, Emmanuel Rivera-Pérez, Antonio Díez & Miguel V. Andrés.

9

- **Metal Oxocluster/Polymer Hybrid Nanoparticles for Heterogeneous Catalysis**
  Hilario Verdeguer-Asensio, Cesare Benedetti, Francisco F. Pérez-Pla, Mauro Carraro, Katharina Landfester, Silvia Gross, Rafael Muñoz-Espí

10

- **Optical fiber amplification of light pulses generated by an ytterbium Mode-Locked laser**
  Antonio Carrascosa, José L. Cruz, Antonio Díez and Miguel V. Andrés

11

- **Thermal Energy Storage in Polymer-Based Micro- and Nanocapsules**
  Adrián Aguado-Hernándiz, Inés Adam-Cervera, Isabel Balaguer-Bernad, Olaia Álvarez-Bermúdez, Katharina Landfester, Rafael Muñoz-Espí

12

- **Graphene/SiC as a Van der Waals substrate for molecular beam epitaxy: spontaneous In or Ga intercalation**
  O. Klymov, N. Garro, A. Cros, N. Feldberg, N. Mollard, H. Okuno, M. Gruart and B. Daudin

13

- **High-pressure high-temperature stability and thermal equation of state of zircon-type ErVO**
  J. Ruiz-Fuertes, D. Martinez-García, T. Marqueño, D. Errandonea, S. MacLeod, T. Bernert, E. Haussühl, D. Santamaria-Perez, J. Ibañez, A. Mallavarapu, S. N. Achary, C. Popescu, M. Bettinelli

14

- **Acoustically tuned multi-channel wavelength modulators for integrated photonics**
  Dominik D. Bühler, A. Crespo-Poveda, Paulo V. Santos, A. Cantarero and M. M. de Lima Jr.

15

- **Chitosan-Based Carriers for Drug Delivery**
  Asmaa Elzayat, Rafael Muñoz-Espí

16

- **Multifunctional Hybrid Colloids: Organics and Inorganics Meet at the Nanoscale**
  Ana Torres-Suay, Sergio García, Maria Gascó, Pablo Martín, Juan F. Ferrer-Crespo, Francisco Pérez-Pla, Olaia Álvarez-Bermúdez, Katharina Landfester, Rafael Muñoz-Espí

17

- **Optical amplification in hollow-core negative-curvature fibers doped with perovskite $CsPbBr_3$ nanocrystals**
  Juan Navarro-Arenas, Isaac Suárez, Albert Ferrando, Andrés F. Gualdrón-Reyes, I. Mora-Seró, Juan Martínez-Pastor, Zhipei Sun

18

- **Metallic nanostructures of metallica**
  Augusto Juste-Dolz, Miquel Avella-Oliver, Ángel Maquieira

19

- **Porosity modulation in mesoporous solids through post-synthetic treatments**
  M. Dolores Garrido, Carolina García-Llácer, Pablo Piqueras, Rahma Hanny, Jamal El Haskouri, José Vicente Ros-Lis, Borja Díaz, Francisco Pérez-Pla, M. Dolores Marcos, Aurelio Beltrán and Pedro Amorós

20

- **Chemical and mechanochemical preparative strategies to control the aggregation level in bimodal mesoporous nanoparticulated silicas**
  Valeriano Bellver, Jamal El Haskouri, José Vicente Ros-Lis, Aurelio Beltrán and Pedro Amorós

Caracterización estadística de ruido de emisión espontánea amplificada de banda angosta

Pablo Muniz-Cánovas[1], Yuri Barmenkov[1,2], Alexander Kir'yanov[1],
José L. Cruz[2], Miguel Andrés[2]

[1)] *Centro de Investigaciones en Óptica, Loma del Bosque 115, 37150, León, Gto. Mexico.*
[2)] *Institut de Ciència dels Materials (ICMUV), Universitat de València, Catedrático José Beltrán 2, 46980 Paterna, Valencia, Spain. Author E-mail: pablomc@cio.mx*

Las fuentes de luz basadas en emisión espontánea estimulada (ASE) se caracterizan por un espectro amplio y una alta estabilidad temporal, que se da por la ausencia de oscilaciones de relajación y efectos de interferencia. La estadística de ruido de una señal de ASE no filtrada se puede modelar usando una de distribución de Poisson; sin embargo, cuando se aplica un filtro de banda angosta la descripción de su estadística de ruido pasa a ajustarse mejor con la distribución de Bose-Einstein con grado de degeneración *M*, como se muestra en la fórmula 1 [1,2] .

$$P(n,\bar{n},M)=\frac{\Gamma(n+M)}{\Gamma(n+1)\Gamma(M)}\left(1+\frac{M}{\bar{n}}\right)^{-n}\left(1+\frac{\bar{n}}{M}\right)^{-M} \qquad (1)$$

Donde *n* es el número instantáneo de fotones, $\bar{n}$ es el promedio total de fotones y *M* corresponde al número de estados independientes de emisión espontánea. Por su parte, el número de fotones se relaciona directamente con la potencia de la señal mediante $n = WT/h\nu$, siendo *W* la potencia óptica, *T* el período de muestreo, *h* la constante de Plank, y ν la frecuencia óptica.

En este trabajo se comparan los resultados teóricos del modelo, con datos experimentales obtenidos a partir de una fuente de semilla de pulsos ASE basada en una cadena de amplificación de erbio, y filtrando la señal mediante el uso de redes de Bragg (FBGs), como se presenta en la Figura 1.

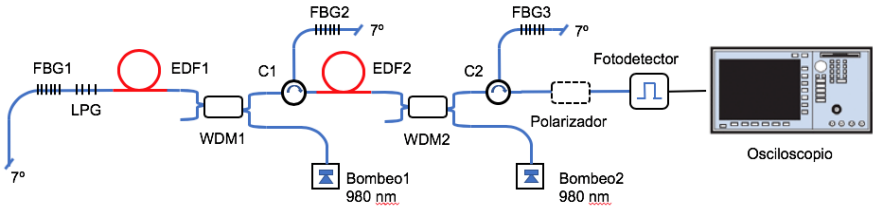

Figura 1. *Arreglo experimental.*

FBG1 y FBG2 son redes de Bragg fijas de 300 pm, mientras que FBG3 cambia en cada prueba, con anchos espectrales que van desde los 20 hasta los 200 picómetros, y que se miden bajo dos esquemas: (1) Osciloscopio de 2.5 GHz y un fotodetector de 5 GHz y (2) Osciloscpio de 16 GHz y fotodetector de 25 GHz. Ambos son presentados tanto para luz polarizada (*s = 1*), así como para luz sin polarización (*s = 2*). En la figura 2 se presenta un ejemplo de la evaluación del modelo para una FBG3 de 76 pm, bajo las condiciones mencionadas.

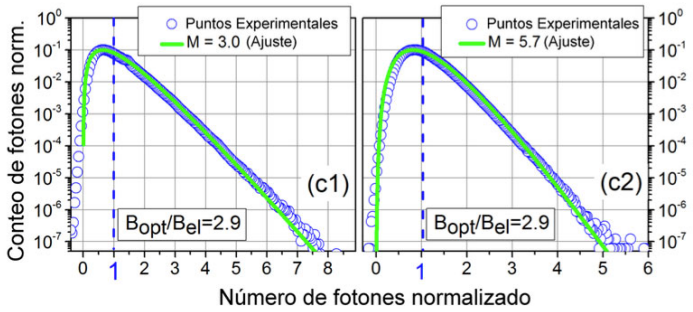

Figura 2. *Muestra de evaluación del modelo, (c1) es el caso polarizado y (c2) el no polarizado .*

Al analizar los diversos casos, se confirma la validez del modelo, así como la dependencia que tiene el número *M* de la relación entre la frecuencia óptica y la frecuencia eléctrica de cada caso. Adicionalmente, se concluye que el número *M* nunca puede llegar a alcanzar el valor unitario y, por tanto, la luz ASE filtrada no puede a su vez adoptar una estadística de fotones perfectamente exponencial.

Referencias

[1] J. W. Goodman, Statistical Optics (Wiley, NY, 2000).
[2] S. M. Pietralunga et al., "Photon statistics of amplified spontaneous emission in a dense wavelength-division multiplexing regime," Opt. Lett. 28, 152-154 (2003).

Polarization Modulation Instability in all-normal Dispersion Microstructured Optical Fibers

A. Loredo-Trejo*, Y. López-Dieguez, A. Díez, E. Silvestre and M. V. Andrés

Departamento de Física Aplicada y Electromagnetismo, Universidad de Valencia, c/ Dr. Moliner 50, 46100, Burjassot, Valencia, España.

**e-mail: abraham.loredo@uv.es*

Introduction.

Polarization modulation instability (PMI) is a form of modulation instability that involves different polarization states of light [1]. In the scalar case, modulation instability (MI) can only exist when the fiber chromatic dispersion is anomalous, and phase matching is achieved by self-phase modulation. However, MI can also occur in normal dispersion when phase matching is accomplished due to cross-phase modulation, specifically, by the coherent coupling between different polarizations components of the light propagating into the fiber. For this phenomenon, the fiber birefringence takes a major role in the phase matching condition. PMI can exist in weakly birefringent fibers, but also in isotropic fibers with almost zero birefringence [2].

In this contribution, we report our results regarding the generation of PMI effect in weakly birefringent, all- normal dispersion (ANDi) microstructured optical fibers (MOFs). In recent years, the nonlinear properties of ANDi MOFs have been deeply investigated, particularly after the generation of coherent, octave-spanning, and recompressible supercontinuum (SC) light was demonstrated using such type of fibers [3].

Methodology and Experimental results

Inset of Fig. 1(a) shows scanning electron microscope (SEM) images of the fibers used in the experiments. Figure 1(a) shows the chromatic dispersion as a function of wavelength, along with theoretical calculations. The dispersion shows the typical convex profile of ANDi fibers with normal dispersion for all wavelengths. The dispersion at 1064 nm is -100 ps/nm km and -21 ps/nm km, for MF1 and MF2, respectively. The fibers were pumped by a microchip Nd:YAG laser that emits linearly polarized pulses of 700 ps duration at 1064 nm. Typical fiber lengths used in the experiments was ~50 cm. A half-wave plate (HWP) was used to rotate the polarization plane of the pump. Figure 1(b) shows the spectrum of the output light for two orthogonal polarization orientations of the pump. Along with the pump laser, we can observe several nonlinear features. For both HWP angles, Stokes and anti-Stokes Raman scattering was generated. Additionally, two narrow bands centered at 1028 nm and 1102 nm, respectively, are shown for just one polarization orientation. Such narrow bands result from a PMI process, specifically, when the fiber is pumped in the slow mode and sidebands are generated in the fast mode.

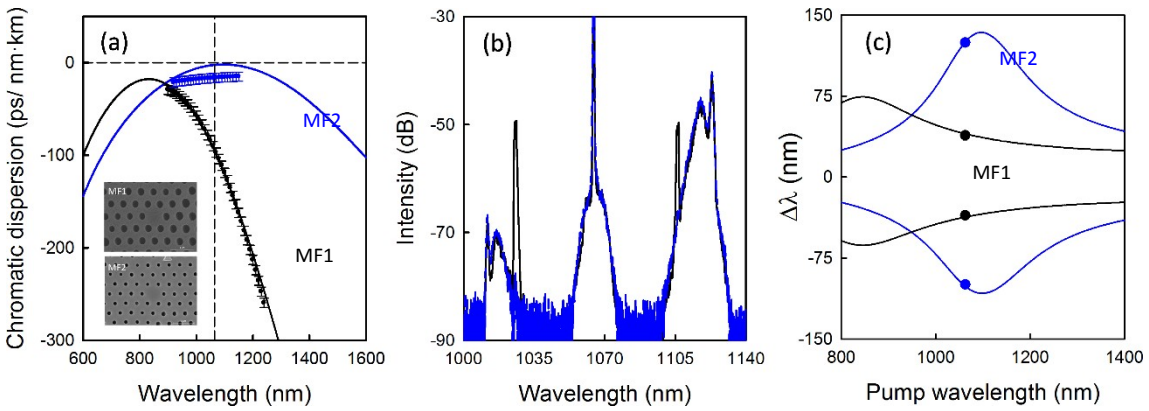

Fig. 1 (a) Chromatic dispersion vs. wavelength of the fibers used in the experiments. Dots are experimental measurements and solid lines are theoretical calculations. Inset: SEM images of the fibers' cross section. MF1: Λ=1 μm, d/Λ=0.52; MF2: Λ=1.6 μm, d/Λ=0.37. (b) Spectra from MF1 for two orthogonal polarizations orientations of the pump. Peak power: 2 kW. (c) Wavelength shift of PMI bands vs. pump wavelength. Theoretical calculations (solid lines), experimental data (dots).

Figure 1(c) shows theoretical calculations of the wavelength shift of PMI bands as a function of pump wavelength. The experimental wavelengths obtained at 1064 nm are also included for both fibers.

References

[1] Agrawal, G. P., Nonlinear Fiber Optics, Academic Press, San Diego (2001).

[2] P. Kockaert, M. Haelterman, S. Pitois and G. Millot, Appl. Phys. Lett., Vol. 75, pp. 2873-2875 (1999).

[3] A. M. Heidt, A. Hartung, G. W. Bosman, P. Krok, E. G. Rohwer, H. Schwoerer, and H. Bartelt, Opt. Express, Vol. 19, pp. 3775-3787 (2011).

Refining two-dimensional semiconductors photoluminescence emission: SiO_2 microspherical resonators in WSe_2 and InSe

Daniel Andres-Penares [1], Juan P. Martínez-Pastor [1], Carlos J. Zapata-Rodriguez [2] and Juan F. Sánchez-Royo [1,*]

[1] *ICMUV, Instituto de Ciencia de Materiales, Universidad de Valencia, P.O. Box 22085, 46071 Valencia, Spain*

[2] *PNO, Group of Plasmonics and Nano-Optics, Department of Optics, University of Valencia, C/ Doctor Moliner 50, Burjassot, 46100 Valencia, Spain*

*E-mail: lowdim@uv.es

Photoluminescence (PL) emission and emitted light management in two-dimensional (2D) semiconductors is a major matter for the implementation of optoelectronic and photonic applications.[1,2] In this sense, several strategies have been considered in order to enhance and tune light emission of 2D semiconductors for a specific device.[3] In this work, SiO_2 microspheres deposited on top of exfoliated 2D nanosheets have been used to enhance the PL of III-VI 2D semiconductors by means of the whispering gallery modes (WGM) in the microspheres. to obtain a fine-tuning of the PL peak wavelength in transition metal dichalcogenides (TMDs), as another degree of freedom for photonic applications, by varying the microsphere diameter. Besides these advantages, microspheres produce a lensing effect of incident laser beam that increases the excitation power density and hence PL intensity on the observation area of the 2D semiconductor, without any change in the laser setup used in the experiment.

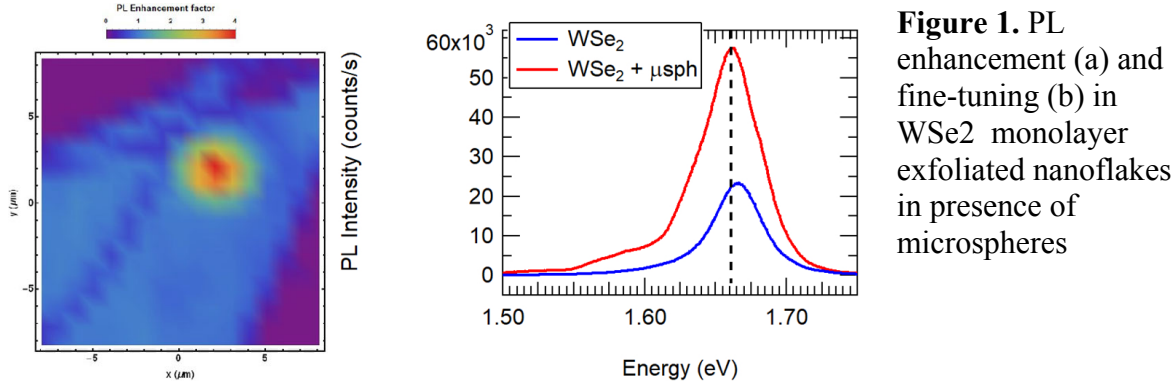

Figure 1. PL enhancement (a) and fine-tuning (b) in WSe2 monolayer exfoliated nanoflakes in presence of microspheres

[1] Huang, J.K.; Pu, J.; Hsu, C.L.; Chiu, M.H.; Juang, Z.Y.; Chang, Y.H.; Chang, W.H.; Iwasa, Y.; et al. Large-area synthesis of highly crystalline WSe2 monolayers and device applications. *ACS Nano* **2014**, *8*, 923–930.

[2] Tonndorf, P.; Schmidt, R.; Böttger, P.; Zhang, X.; Börner, J.; Liebig, A.; Albrecht, M.; Kloc, C.; Gordan, O.; Zahn, D.R.T.; et al. Photoluminescence emission and Raman response of monolayer MoS2, MoSe2, and WSe2. *Adv. Mater.* **2017**, *29*, 4908–4916.

[3] Brotons-Gisbert, M.; Andres-Penares, D.; Suh, J.; Hidalgo, F.; Abargues, R.; Rodríguez-Cantó, P.J.; Segura, A.; Cros, A.; Tobias, G.; Canadell, E.; et al. Nanotexturing To Enhance Photoluminescent Response of Atomically Thin Indium Selenide with Highly Tunable Band Gap. *Nano Lett.* **2016**, *16*, 3221–3229.

All-polarization-maintaining mode-locked thulium-doped fiber laser

L.A. Sánchez, A. Carrascosa, L. Escalante-Zárate, J.L. Cruz, A. Díez, and M.V. Andrés

Department of Applied Physics and Electromagnetism-ICMUV, University of Valencia, C/ Dr. Moliner 50, Burjassot 46100, Spain. E-mail: luis.sanchez@uv.es

Thulium-doped fiber lasers (TDFLs) have seen growth during the last decades thanks to its wide gain spectrum around 2 μm and the availability of high brightness 790 nm diodes, which allow high efficient cladding pump through a cross relaxation process [1]. Mode-locked TDFLs using passive mode-locking through saturable absorbers have become the most attractive pulsed fiber light source at 2 μm due to the fast response of these absorbers. Narrow band sources at 2 μm with pulses in the order of picoseconds provide high spectral resolution for applications like optical parametric oscillators and Raman microscopy [2].

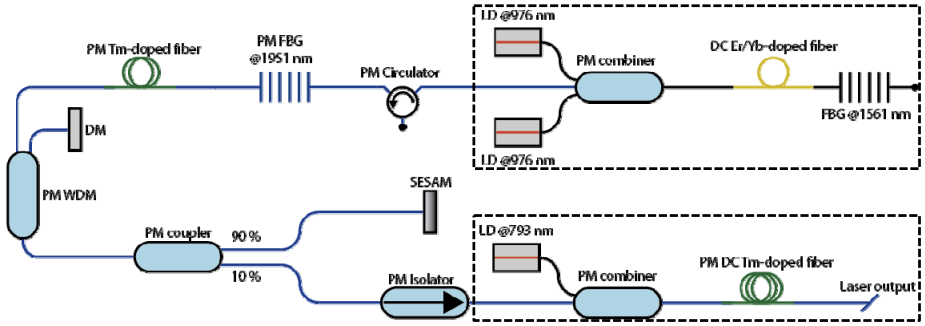

Fig. 1: *Experimental setup of the all-polarization-maintaining thulium-doped fiber laser oscillator. The upper box indicates the pump laser. The lower box indicates the amplifier.*

Here, we show a mode-locked all-fiber thulium-doped laser with polarization preservation through the use of polarization-maintaining (PM) fiber and components. The experimental setup of the laser is shown in Fig.1. The TDFL was pumped by a homemade continuous wave all-fiber laser emitting at the C band. The TDFL cavity was formed by a narrow-band PM FBG and a semiconductor saturable absorber mirror (SESAM). The Bragg wavelength of the PM FBG was 1951 nm and its reflectivity was estimated to be >99% for the slow axis. The laser gain is provided by 2 m-long PM Tm-doped fiber. Passively mode-locking was provided using the SESAM coupling it to the 90% arm of a 90/10 PM output coupler. This coupler filtered the fast axis polarization so that the slow axis polarization was amplified. Excellent temporal stability was achieved due to the single polarization operation. Pulses from the oscillator were amplified by one-stage PM thulium-doped fiber amplifier. The amplifier consists of a 4.5 m-long double cladding PM Tm-doped fiber, a 793 nm laser diode up to 7.7 W and a PM combiner.

Mode-locking self-started at an incident 1561 nm pump power of 350 mW. The oscillator delivered pulses with a repetition frequency of 16.43 MHz. The slope efficiency of the amplification stage was 38.75%. Amplified spontaneous emission (ASE) was observed in the output spectrum. The ratio between the laser peak and the maximum of ASE was 46 dB. The 10 dB spectral bandwidth varied between 250 and 500 pm as function of the amplifier pump power due to self-phase modulation. The pulse duration was estimated to be below 85 ps.

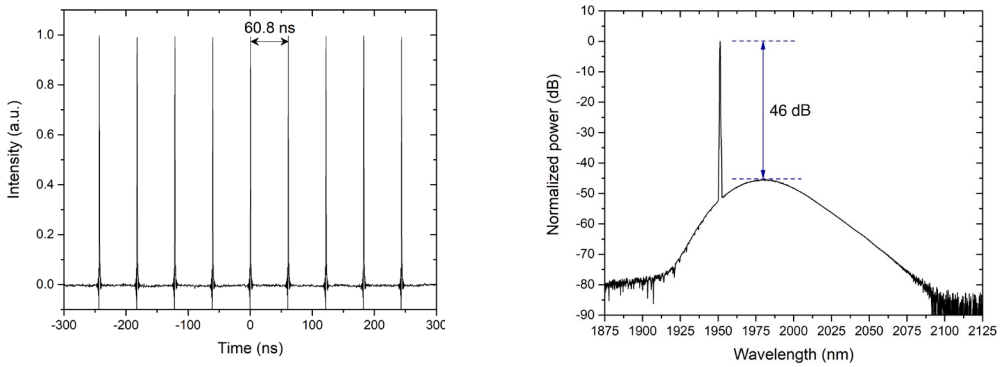

Fig. 2: *(a) Pulse train of the passively mode-locked TDFL. (b) Spectrum after the amplifier stage for an output power of 1.2 W.*

References

[4] Yulong TANG, Chongyuan HUANG, Shengli WANG, Hongqiang LI, and Jianqiu XU, *"High-power narrow-bandwidth thulium fiber laser with an all-fiber cavity"*, Opt. Express, 20, 17539-17544, 2012.

[5] Yue ZHOU, Kim K. Y. CHEUNG, Sigang YANG, P. C. CHUI, Kenneth K. Y. WONG, *"Ultra-Widely tunable, narrow linewidth picosecond fiber-optical parametric oscillator"*, IEEE Photonics Technology Letters, 22(23), 1756–1758, 2010.

High-pressure characterization of the optical and electronic properties of InVO4, InNbO4, and InTaO4

P. Botella[1], D. Errandonea[2], A. B. Garg[3,4], P. Rodriguez-Hernandez[5], A. Muñoz[5], S. N. Achary[6], A. Vomiero[1]

[1] *Department of Engineering Sciences and Mathematics Luleå University of Technology, SE-97187 Luleå, Sweden*
[2] *Departamento de Física Aplicada-Instituto de Ciencia de Materiales,MALTA ConsoliderTeam, Universidad de Valencia, Edificio de Investigacion, C/Dr. Moliner 50, Burjassot, 46100 Valencia, Spain*
[3] *High Pressure and Synchrotron Radiation Physics Division, Bhabha Atomic Research Centre, Mumbai 400085, India*
[4] *Homi Bhabha National Institute, Anushakti Nagar, Mumbai 400094*
[5] *Instituto de Materiales y Nanotecnología, Departamento de Física, MALTA ConsoliderTeam, Universidad de La Laguna, La Laguna, E-38205 Tenerife, Spain*
[6] *Chemistry Division, Bhabha Atomic Research Centre, Trombay, Mumbai 400085, India*

Abstract

We have studied the electronic properties at ambient pressure and under high pressure of $InVO_4$, $InNbO_4$, and $InTaO_4$ powders, three candidate materials for hydrogen production by means of photocatalytic water splitting using solar energy.[1,2] A combination of optical absorption and resistivity measurements and band structure calculations have allowed us to determine that these materials are wide band-gap semiconductors with a band-gap energy of 3.62(5), 3.63(5), and 3.79(5) eV for $InVO_4$, $InNbO_4$, and $InTaO_4$, respectively. The last two compounds are indirect band-gap materials, and $InVO_4$ is a direct band-gap material.[3-5] The pressure dependence of the band-gap energy and the electrical resistivity have been determined too. In the three compounds, the band gap opens under compression until reaching a critical pressure, where a phase transition occurs. The structural transition triggers a band-gap collapse larger than 1.2 eV in the three materials, being the abrupt decrease in the band-gap energy related to an increase in the pentavalent cation coordination number. The phase transitions also cause changes in the electrical resistivity, which can be correlated with changes induced by pressure in the band structure. An explanation to the reported results is provided based upon ab initio calculations. The conclusions attained are of significance for technological applications of the studied oxides.

References

[1] M. Oshikiri, M. Boero, J. Ye, Z. Zou, and G. Kido, Electronic structures of promising photocatalysts $InMO_4$ (M = V, Nb, Ta) and $BiVO_4$ for water decomposition in the visible wavelength region, J. Chem. Phys. **117**, 7313 (2002).

[2] J. Ye, Z. Zou, H. Arakawa, M. Oshikiri, M. Shimoda, A. Matsushita, and T. Shishido, Correlation of crystal and electronic structures with photophysical properties of water splitting photocatalysts $InMO_4$ (M= V^{5+}, Nb^{5+}, Ta^{5+}), J. Photochem. Photobiol. A Chem. **148**, 79 (2002).

[3] D. Errandonea, C. Popescu, A. B. Garg, P. Botella, D. Martinez-García, J. Pellicer-Porres, P. Rodríguez-Hernández, A. Muñoz, V. Cuenca-Gotor, and J. A. Sans, Pressure-induced phase transition and band-gap collapse in the wide-band-gap semiconductor $InTaO_4$, Phys. Rev. B **93**, 1 (2016).

[4] A. B. Garg, D. Errandonea, C. Popescu, D. Martinez-García, J. Pellicer-Porres, P. Rodríguez-Hernández, A. Muñoz, P. Botella, V. P. Cuenca-Gotor, and J. A. Sans, Pressure-Driven Isostructural Phase Transition in $InNbO_4$: In Situ Experimental and Theoretical Investigations, Inorg. Chem. **56**, 5420 (2017).

[5] D. Errandonea, O. Gomis, B. García-Domene, J. Pellicer-Porres, V. Katari, S. N. Achary, A. K. Tyagi, and C. Popescu, New Polymorph of $InVO_4$: A High-Pressure Structure with Six-Coordinated Vanadium, Inorg. Chem. **52**, 12790 (2013).

Printed luminescent chemosensor for detection of nitroderivate compounds

Eduardo Aznar [1], Rafael Abargues [1], Juan P. Martínez-Pastor [1], Pedro Rodríguez-Cantó [2*] [1] *Institut de Ciència dels Materials (ICMUV), Universitat de València, Catedrático José Beltrán 2, 46980 Paterna, Valencia, Spain*
[2] *INTENANOMAT S.L., C/ Catedrático José Beltrán 2, 46980 Paterna, Spain.*

*E-mail: azgae@uv.es

The role of nanoscience in analytical science has been greatly established for the development of chemical sensors with enhanced performance. The design of low-cost, easy-to-fabricate and portable analytical devices with a low limit of detection (LOD), good selectivity, high sensitivity and short response time are in high demand.[1,2,3] In this sense, chemical sensors based on fluorescent quantum dots (QDs) have attracted intense interest because of their excellent optical and electronic properties compared to the routinely employed fluorescent organic dyes.[4] These properties include size-tunable light emission over a wide range of energies, high photoluminescence quantum yield (PL QY), narrow emission line width, and good solution processability.[5] In addition, the physicochemical stability of QDs, their extremely large surface area, as well as the possibility of functionalizing their surface by conjugation with appropriate molecules make them very attractive nanomaterials for ultrasensitive sensors with the possibility of multiplex chemical detection.[6]

In this work, we have developed a novel CdSe QD-polymer-based luminescent chemosensor for the selective detection of explosive or explosive-like molecules. The sensor is based on an array pattern containing either green-emitting or red-emitting CdSe QDs in polycaprolactone (PC) as a polymer host matrix. Here, the sensor fabrication is performed by a microplotter, a direct printing technique based on ultrasonic fluid microdispensing to generate the nanocomposite patterning, resulting in accurate and high-resolution patterns. The transduction mechanism of the sensor is based on changes of the QD photoluminescence (PL) when molecules are adsorbed on the QD surface.

We evaluate the sensing capability of the nanocomposites by exposing the patterns to vapours of some high explosive or explosive-like molecules. Additionally, two different molecules such as 2- mercaptoethanol (MET) and ethylenediamine (EDA) are also tested for comparison. Remarkably, the change in intensity and response times for this two nanocomposites are quite varied depending upon the analyte to which it is exposed. The LOD of the sensors was determined to be as low as 10^{-10} M for all analytes. Monitoring the changes in the fluorescence intensities of both nanocomposite patterns allows to pin-point each analyte on a two-dimensional (2D) map, where selectivity can be greatly enhanced.

We believe that this type of miniaturized luminescent QD-based nanocomposites might form the basis of a fully disposable sensing platform technology to perform effective chemical sensing and detection of many high explosive or explosive-like molecules among others.

References

[1] F. S. Ligler, Anal. Chem., 2009, 81, 519.
[6] R. Abargues, P. J. Rodriguez-Canto, S. Albert, I. Suarez and J. P. Martínez-Pastor, J. Mater. Chem. C, 2014, 2, 908.
[7] P. J. Rodríguez-Cantó, R. Abargues, H. Gordillo, I. Suárez, V. Chirvony, S. Albert, J. Martínez-Pastor, RSC Adv. 2015, 5, 19874.
[8] U. Resch-Genger, M. Grabolle, S. Cavaliere-Jaricot, R. Nitschke and T. Nann, Nat. Methods, 2008, 5, 763.
[9] Nanocrystal Quantum Dots, ed. V. I. Klimov, CRC Press, Boca Raton, FL, 2nd edn, 2010.
[10] M. F. Frasco and N. Chaniotakis, Sensors, 2009, 9, 7266.

Multi-analytical characterization of Valencian artists' palette from the XIX-XX centuries.

Silvia Caravá[1], Francesca C. Izzo[1], Clodoaldo Roldán García[2],
María Luisa Vázquez de Agredos Pascual[3], Sonia Murcia Mascarós[2]

[1)]*Università Ca' Foscari, Dorsoduro 3246, 30123 Venezia, Italy.*

[2)]*Instituto de Ciencia de los Materiales (ICMUV), Universidad de Valencia, Catedrático José Beltrán 2, 46980 Paterna, Valencia, Spain.*

[3)]*Departamento de Historia del Arte. Universidad de Valencia, Avenida Blasco Ibáñez 28, 46010 Valencia, Spain.*

We present a multi-analytical approach for the characterisation of pigments used in six oil paintings from the *Escuela de Arte y Superior Diseño* (EASDE) of Valencia. The selected artworks were painted between 1871 and 1943 by four Valencian famous artists and have been analysed here for the first time. This work is focused on the palettes' identification by in situ non-invasive techniques (VIS Reflectance and X-ray fluorescence spectrometry), combined with micro-invasive (Optical Microscopy, μ-Raman and ATR-FTIR spectroscopies) and micro-destructive (Gas Chromatography-Mass Spectrometry) techniques.

The results revealed the use of traditional pigments as vermillion, earth pigments, lead white and modern pigments as zinc white, cobalt-based pigments, chromium-based pigments and cadmium yellow, among a huge variety of pigments. The analysis identified fillers and degradation products as calcite, barite, calcium sulphate, lead sulphate and Zn-Pb metal carboxylates, oils and Arabic gum as binding media.

This study provides important information on painters' palette and their artistic production technique and allows underlining the differences between palettes of each artist. Besides, this work highlights the necessity of a multi-analytical approach to identify traditional and modern pigments and to obtain valuable information for documentation and preventive conservation.

Characterization of optical fibers photosensitivity by means of in-fiber acousto-optic interaction

Saúl Rosales-Mendoza, Martina Delgado-Pinar, José Luis Cruz, Emmanuel Rivera-Pérez, Antonio Díez & Miguel V. Andrés.

Laboratory of fiber optics, ICMUV – Applied Physics Department, University of Valencia
C/Dr Moliner, 50, 46100 Burjassot (Valencia) Spain

Abstract. When silica optical fibers are irradiated with UV light, its core refractive index changes due to the photosensitivity of the material. In this work, we quantify the core numerical aperture increase δNA, as a function of the incident UV fluence E (energy per unit area) in a hydrogenated telecom fiber (SMF-28), using in fiber acousto-optic interaction (AOI) as the sensing tool.

Basis

An acoustic wave propagating in an optical fiber stretches and compresses periodically the fiber. Due to the elasto-optic effect, this acoustic wave induces a periodic modulation in the refractive index of the fiber. In presence of this modulation, the optical co-propagating modes can exchange energy, in a resonant way (see figure 1a), at those wavelengths that satisfy the phase matching condition of acousto-optic interaction (AOI):

$$\lambda_R = \Lambda(n_{eff,k} - n_{eff,j}) \qquad (1)$$

where Λ is the period of the refractive index modulation (i.e. the acoustic wavelength), $n_{eff,m}$ is the effective index of the m-th optical mode and λ_R is the resonance optical wavelength which is then a function of the fiber parameters and the acoustic frequency, F, through the optical and acoustic modes dispersion curve. For this reason the characterization in detail of the AOI phase-matching wavelength, λ_R, as a function of F, allows obtaining information about the core radius and numerical aperture of optical fibers (see figure 1b).

Results

The experimental setup is similar to that shown in [1]. In our case, half of the interaction length of fiber was irradiated with a given UV fluence E, half was pristine fiber. When the AOI occurs at a convenient F, two main notches are observed due to the coupling $LP_{01} \rightarrow LP_{11}$. The notch at shorter wavelengths corresponds to the coupling between the modes propagating along the pristine section of the fiber. The redshifted notch corresponds to the same coupling, but along the irradiated section of fiber (see Fig. 1a). By means of the measurement of the phase-matching curve of the coupling, and using Eq. 1 to evaluate the core numerical aperture increase, a measurement of δNA in a broadband can be performed (see Fig. 1b). The evaluation of the increment δNA was measured as a function of the UV fluence, at 1.55 mm, see Fig. 1.c.

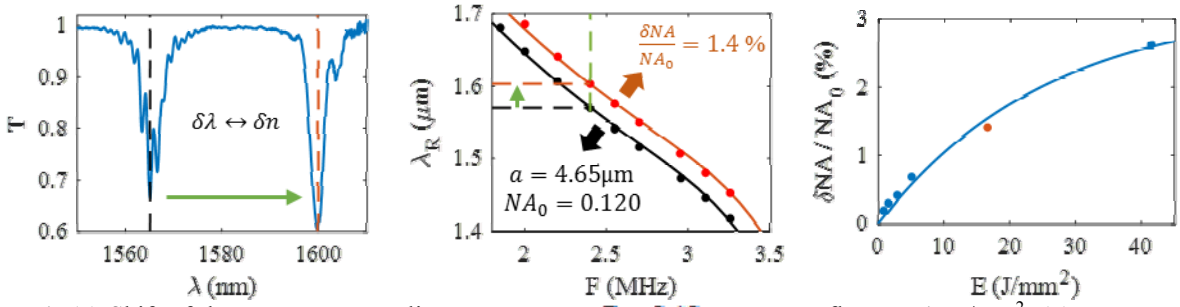

Figure 1. (a) Shift of the LP_{01}-LP_{11} coupling resonance at $F = 2.42$ MHz. UV fluence: 17 J/mm^2. **(b)** Measured (dots) and calculated (solid curve) phase-matching tuning curve for the pristine section (black) and the irradiated section (red). **(c)**Numerical aperture increase as a function of UV fluence (dots) and exponential fit (solid line). The red dot corresponds to the fiber characterized in figures (a) and (b).

References

[1] E. Alcusa-Sáez, A. Diez & Miguel V. Andrés (2016). Optic Express, **24**(5), 4899-4905

Metal Oxocluster/Polymer Hybrid Nanoparticles for Heterogeneous Catalysis

Hilario Verdeguer-Asensio,[1,*] Cesare Benedetti,[2] Francisco F. Pérez-Pla,[1] Mauro Carraro,[3] Katharina Landfester,[2] Silvia Gross,[3] Rafael Muñoz-Espí[1]

[1)] *Institut de Ciència dels Materials (ICMUV), Universitat de València, Paterna, Spain*

[2)] *Max Planck Institute for Polymer Research, Mainz, Germany*

[3)] *Dipartimento di Scienze Chimiche, Università degli Studi di Padova, Padova, Italy*

*E-mail: hivera@alumni.uv.es

Miniemulsion polymerization is a very versatile technique to prepare a large variety of polymer and hybrid nanoparticles [1]. By using this technique, functionalized inorganic building blocks (such as oxoclusters with polymerizable moieties) can be incorporated into a polymer matrix through copolymerization with suitable monomers [2, 3].

This work focuses on the synthesis of hybrid poly(methyl methacrylate) nanoparticles, cross-linked with hafnium, zirconium, and titanium oxoclusters, namely $Hf_4O_2(OMc)_{12}$, $Zr_4O_2(OMc)_{12}$, and $Ti_4O_2(O^iPr)_6(OMc)_6$ (OMc = methacrylate), by means of miniemulsion polymerization. The oxoclusters contain double bonds able to copolymerize with a vinyl monomer (methyl methacrylate). The nanoparticles are applied as heterogeneous catalysts for the oxidation of organic sulfides. The results obtained with hafnium, zirconium, and titanium oxoclusters are compared.

The formation of covalent bonds between the organic and the inorganic part provides structural stability. The particle size increases as the amount of introduced oxocluster increases. As a result of cross-linking, the nanoparticles are insoluble in organic solvents, but they swell and increase their size significantly. This swelling allows for the use of the particles as heterogeneous catalysts, since the catalytic active centers of the oxoclusters become accessible.

[1] M. A. Hood, M. Mari, R. Muñoz-Espí. *Materials* **2014**, *7*, 4057–4087.

[2] C. Benedetti, A. Cazzolaro, M. Carraro, R. Graf, K. Landfester, S. Gross, R. Muñoz-Espí, *ACS Appl. Mater. Interf.* **2016**, *8*, 26275–26284.

[3] C. Benedetti, P. Flouda, A. Antonello, C. Rosenauer, F. F. Pérez-Pla, K. Landfeser, S. Gross, R. Muñoz-Espí, Nanotechnology **2017**, *28*, 365603 (8 pp).

Optical fiber amplification of light pulses generated by an ytterbium Mode-Locked laser

Antonio Carrascosa*, José L. Cruz, Antonio Díez and Miguel V. Andrés

Department of Applied Physics and Electromagnetism-ICMUV, University of Valencia, C/Dr. Moliner 50, Burjassot 46100, Spain

*E-mail: antonio.carrascosa@uv.es

Mode-locked lasers developed in Ytterbium doped fiber have proved to be a very robust tool for scientific and industrial applications [1]. Among the industrial applications it can highlighted materials processing, marking engraving and LIDAR; in the scientific field must be mentioned signal processing, the CARS microscopy or super-continuum generation [2, 3, 4].

We are developing a passively mode-locked (ML) fiber laser where all components used are made in optical fiber technology (figure 1). The gain medium is an ytterbium doped fiber, modulation to get pulsed emission is generated by a saturable absorbed and an acousto-optic modulator is used as pulse rate selector. This work shows the main laser characteristics focusing on stability, output power and optical spectrum, which are dependent on the pump power and the active fiber length (PM LMA Yb) of the power amplifier.

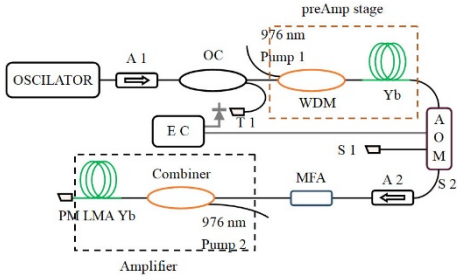

Figure 1: Laser set-up

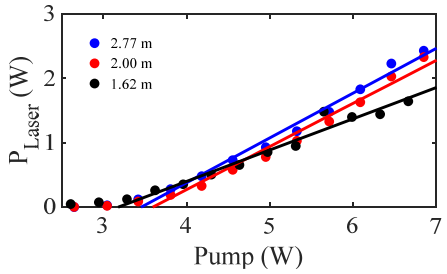

Figure 2: Laser power as function of pump power for different lengths of active fiber.

The figure 2 shows the laser output power as a function of pump power, high effficiency is achieved for large lengths of fiber with a pump threshol of 3W. Figure 3 shows the laser spectrum for a pump power of 6.5 W; the corresponding outpup peak powers are 147 kW a fiber lenfth of 2.77m and 157 KW for fiber lengths of 1.6 m or 2 m.

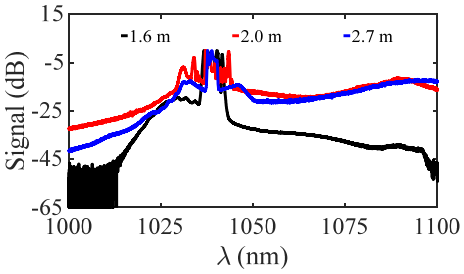

Figure 3: Laser spectrum as for different lengths of active fiber.

[1] Martin E. Fermann and Ingmar Hartl. *Ultrafast fibre lasers*. Nature Photonics volume 7, 868 – 874, 2013.

[2] L. J. Poveda-Wong, A. Carrascosa, C. A. Cuadrado-Laborde, J. L. Cruz, A. Díez y M. V. Andrés. *Long-period grating assisted fractional differentiation of highly chirped light pulses*. Optics Communications, Vol. 363, 37 - 41, 2016.

[3] Baumgartl M, Gottschall T, Abreu-Afonso J, Díez A, Meyer T, Dietzek B, Rothhardt M, Popp J, Limpert J, Tünnermann A. *Alignment-free, all-spliced fiber laser source for CARS microscopy based on four-wave-mixing*. Opt Express 20 (19). 2012

[4] S. Kivistö, R. Herda, and O. G. Okhotnikov. *All-fiber supercontinuum source based on a mode-locked ytterbium laser with dispersion compensation by linearly chirped Bragg grating*. Optics Express 16, 1, 265-270, 2008.

Thermal Energy Storage in Polymer-Based Micro- and Nanocapsules

Adrián Aguado-Hernándiz[1], Inés Adam-Cervera[1], Isabel Balaguer-Bernad[1], Olaia Álvarez-Bermúdez[1,2], Katharina Landfester[2], Rafael Muñoz-Espí[1,*]

1) *Institut de Ciència dels Materials (ICMUV), Universitat de València, Catedrático José Beltrán 2, 46980 Paterna, Valencia, Spain*

2) [2)] *Max Planck Institute for Polymer Research, Ackermannweg 10, 55128 Mainz, Germany*

*rafael.munoz@uv.es

Energy storage systems are necessary to face the chronological mismatch between production and demand that renewable energies constantly suffer from. A promising contribution, object of current investigation, is the use of solid–liquid phase-change materials (PCMs), which store thermal energy in form of latent heat during the melting process and recover it during recrystallization [1]. PCMs are usually encapsulated to ensure the cyclability of the process, to avoid leakage, and to protect the surrounding media from negative effects, such as corrosion [2].

In this work, we present the encapsulation of hydrophilic and hydrophobic PCMs in hybrid capsules formed by a polymer and metal oxides *via* different colloidal techniques. On the one hand, hydrated inorganic salts are encapsulated in polyurethane systems prepared by polyaddition in inverse miniemulsion, estabilized by the Pickering method with magnetite nanoparticles. On the other hand, alkanes and fatty acids are encapsulated in polystyrene systems prepared by radical polymerization in direct miniemulsion.

The ability to store thermal energy of the different systems prepared was studied by differential scanning calorimetry (DSC). Supercooling problems (i.e., crystallization at significantly lower temperature than the melting point), common in PCMs, were corrected by the co-encapsulation of small amounts of a nucleating agent. The storage of thermal energy is efficient and reproducible after a large number of cycles.

References:

[1] Schoth, A.; Landfester, K.; Muñoz-Espí, R. *Langmuir* **2015**, *31*, 3784–3788.

[2] Milián, Y. E.; Gutiérrez, A.; Grágeda, M.; Ushak, S. *Renew. Sust. Energ. Rev*. **2017**, *73*, 983–999.

[3] Schoth, A.; Keith, A. D.; Landfester, K.; Muñoz Espí, R. *RSC Adv.* **2016**, *6*, 53903–53911.

Graphene/SiC as a Van der Waals substrate for molecular beam epitaxy: spontaneous In or Ga intercalation

O. Klymov[1], N. Garro[1], A. Cros[1], N. Feldberg[2,3], N. Mollard[2], H. Okuno[2], M. Gruart[2] and B. Daudin[2]

[1]Institute of Materials Science (ICMUV), University of Valencia, PO Box 22085, E-46071, Valencia, Spain

[2]Université Grenoble Alpes, CEA, INAC, F-38054 Grenoble Cedex 9, France

[3]CEA, LETI, MINATEC campus, 38000 Grenoble, France10)

*E-mail: nuria.garro@uv.es

The use of graphene as a substrate in epitaxial growth is attracting great attention based on the clear benefits of graphene transparency, high conductivity and flexibility as well as on the Van der Waals character of its interaction with the material. Nevertheless, the effects of epitaxial growth on the properties of graphene are poorly understood. In this work we analyze epitaxial graphene on (0001) SiC before and after being used as a substrate for the growth of GaN by plasma-assisted molecular beam epitaxy. We report on the formation of a self-limited Ga or In metallic bilayer which gets intercalated between graphene and the SiC surface by diffusion at SiC steps. The role of N and Ga deposition on the characteristics of graphene are investigated in different samples. The structural changes under the different treatments are addressed by Atomic Force Microscopy (AFM), and correlated with the electrical properties of the 2D layer by Kelvin Probe Force Microscopy (KPFM). Strain and doping of the graphene layers were analyzed by Raman scattering maps. The results obtained indicate that the intercalation of N or metal species between graphene and SiC takes place only in one-layer graphene regions, leading to the full decoupling of graphene from the SiC surface. When effectively detached from SiC, graphene decreases its doping level and improves considerably both strain and doping homogeneity.

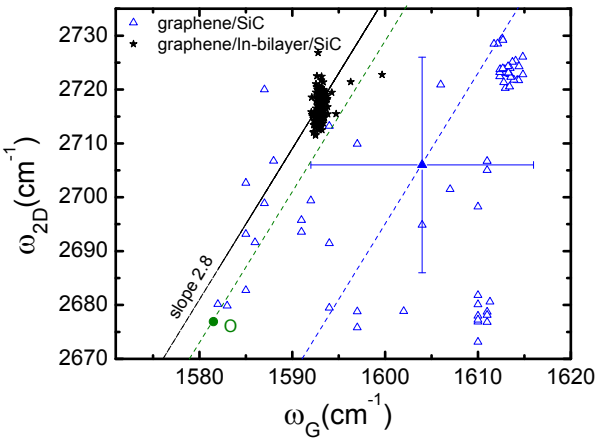

Figure 1: Variation of the 2D peak frequency as a function of the G peak frequency for different samples.

High-pressure high-temperature stability and thermal equation of state of zircon-type $ErVO_4$

J. Ruiz-Fuertes[1], D. Martinez-García[2], T. Marqueño[2], D. Errandonea[2], S. MacLeod[3,4], T. Bernert[5], E. Haussühl[6], D. Santamaria-Perez[2], J. Ibañez[7], A. Mallavarapu[8], S. N. Achary[9], C. Popescu[10], M. Bettinelli[11]

1. DCITIMAC, Universidad de Cantabria, Avenida Los Castros 48, 39005 Santander, Spain

2. Departament de Física Aplicada, Universitat de Valencia, Dr. Moliner 50, 46100 Burjassot, Spain.

3. Atomic Weapons Establishment, Aldermaston, Reading RG7 4PR, United Kingdom.

4. SUPA, School of Physics & Astronomy, and Centre for Science at Extreme Conditions, The University of Edinburgh, Edinburgh EH9 3FD, United Kingdom.

5. Max-Planck-Institut für Kohlenforschung, Kaiser-Wilhelm-Platz 1, 45470 Mülheim an der Ruhr, Germany.

6. Institut für Geowissenshaften, Goethe-Universitat Frankfurt, Altenhöferallee 1, 60438 Frankfurt am Main, Germany.

7. Institute of Earth Sciences Jaume Almera, CSIC, 08028 Barcelona, Spain

8. Material Processing & Corrosion Engineering Division, Bhabha Atomic Research Centre, Trombay, Mumbai 400085, India.

9. Chemistry Division, Bhabha Atomic Research Centre, Trombay, Mumbai 400085, India.

10. CELLS-ALBA Synchrotron Light Facility, Cerdanyola del Vallès, 08290 Barcelona, Spain.

11. Laboratorio Materiali Luminescenti, DB, Universitàdi Verona, and INSTM, UdR Verona, 37134 Verona, Italy.

Abstract

The accurate determination of the phase diagram and high-temperature equation of state (EOS) of zircon-type vanadates is crucial in the design of composites and nanoparticles. Zircon-type vanadates undergo to an irreversible phase transition to a scheelite-type structure at moderate pressures. However, with a unit-cell volume collapse of around 10%, the crystallinity of the scheelite-type phase is compromised when the transformation is induced at room temperature. This drawback can be overcome by inducing the phase transition at high pressure and high temperature. Here we present *in situ* high pressure and room temperature single crystal x-ray diffraction (XRD) and high-pressure and high-temperature powder XRD studies with a diamond anvil cell up to 20 GPa and 700 K, as well as an ex situ powder XRD study with a Paris-Edinburgh cell at 4 GPa and temperatures up to 1300 K. The results show that $ErVO_4$ transforms at room temperature to the scheelite phase at 8.3 GPa remaining stable at least up to 20 GPa. Otherwise, at 4 GPa $ErVO_4$ starts transforming to the scheelite phase already at 773 K and at 973 when vanadium reduces from V^{5+} to V^{4+} and V^{3+} forming perovskite-type $ErVO_3$ and pyrochlore-type $Er_2V_2O_7$. Our results show the narrow scheelite-phase region of $ErVO_4$ at low pressures and the analysis of the thermal EOS of zircon-type $ErVO_4$ evidence the usual low thermal expansion of vanadates.

Acoustically tuned multi-channel wavelength modulators for integrated photonics

Dominik D. Bühler[1*], A. Crespo-Poveda[1], Paulo V. Santos[2], A. Cantarero[3] and M. M. de Lima Jr.[1]

1) Institut de Ciència dels Materials (ICMUV), Universitat de València, Catedrático José Beltrán 2, 46980 Paterna, Valencia, Spain

2) Paul-Drude-Institut für Festkörperelektronik, Hausvogteiplatz 5-7, 10117 Berlin, Germany

3) Instituto de ciencia molecular (ICMOL), Universitat de València, Catedrático José Beltrán 2, 46980 Paterna, Valencia, Spain

*dominik.buhler@uv.es

We investigate designs for an acoustically tuneable arrayed waveguide grating (AWG) system for the application as optical networking devices that enable wavelength routing and switching among other possible functionalities. We will explore three types of robust, compact and fast responding devices beyond recently demonstrated concepts based on an array of ridge single-mode waveguides tuned by a standing surface acoustic wave (SAW). A light signal with a small bandwidth around the telecommunication wavelength of 1550 nm is introduced laterally into the photonic circuit fabricated in (Al)GaAs material platform. Guided by mono-mode waveguides, the light signal reaches a multimode interference (MMI) device where the signal is split into up to 5 separate outputs forming an array waveguide grating (AWG) in which an incremental length between each waveguide introduces a linear phase-shift. Recombined in a second MMI, these phase-shifts allow us to calculate the demultiplexing of the initial signal so that certain wavelengths are focused to determined spatial output positions. A standing SAW working in the low GHz range can now be used to dynamically control this phasar. The SAW is generated by two interdigital transducers (IDT) that are placed opposite to each other, perpendicular to the AWG, enabling the modification of the refractive index of each arm due to the acousto-optic effect. As a result, the SAW modulation introduces a controlled additional phase shift in every waveguide arm. In this way, the signals can be routed between the different output ports with response times of the order of a few nanoseconds.

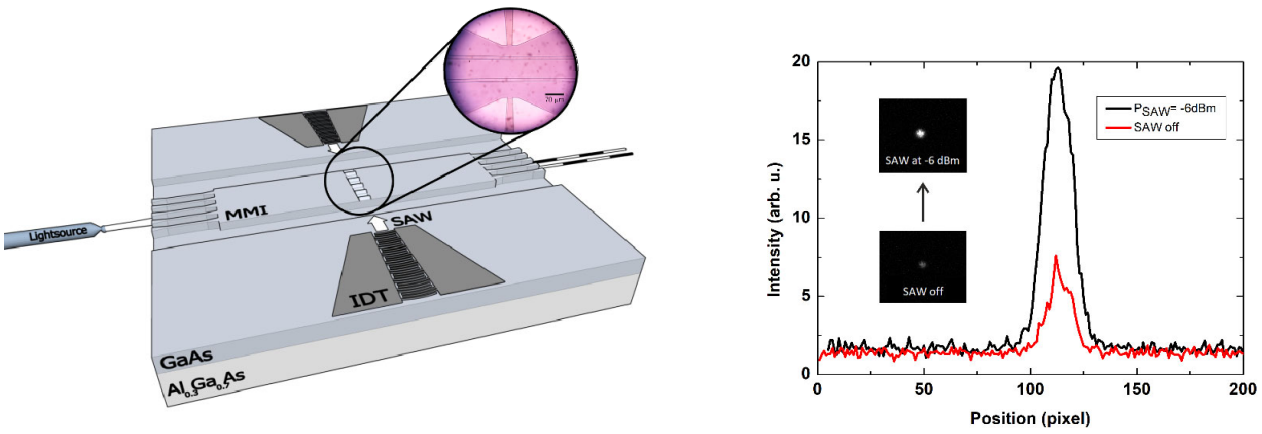

Figure 1 & 2 Concept design (left) and measured response (right) of a single multimode interference based modulator dynamically tuned by a focused surface acoustic wave.

Chitosan-Based Carriers for Drug Delivery

Asmaa Elzayat[1,2], Rafael Muñoz-Espí[1]

[1)] *Institut de Ciència dels Materials (ICMUV), Universitat de Valencia, Paterna, Valencia, Spain.*

[2)] *Faculty of Science, Mansoura University, Mansoura, Egypt.*

E-mail: asmaa.elzayat@ext.uv.es

Controlling the release of pharmaceutical compounds to specific action sites, with increased therapeutic benefit and minimized side effects or toxicity, is a major challenge in designing biomedical micro- and nanocarriers. In recent years, biodegradable polymeric materials have attracted more attention as drug carriers. Encapsulation of drugs in polymers plays an important role in increasing the stability of drugs by protecting them from degradation, but it is also useful to control the release of the drug [1].

In this work, we aim to prepare chitosan carriers by using emulsification methods, studying thereby their efficiency for entrapping drugs and delivering them to a specific target with optimal rate and dose regimen [2]. Chitosan is an attractive biomaterial due to its characteristic chemical and biological properties; it is biocompatible, biodegradable, and nontoxic.

Depending on the preparation technique, we can control the particle size at micro- and nanoscale through an ionic cross-linking mechanism. In contrast to macroscopic systems, nanoparticles could potentially promote an effective permeation through cell membranes and increase the stability in the blood stream.

[1] M. Dash, F. Chiellini, R.M. Ottenbrite, E.Chiellini. *Prog. Polym. Sci.* **2011**, *36*, 981-1014.

[3] M.A. Hood, K. Landfester, R. Muñoz-Espí. *Colloids Surf. A* **2018**, *504*, 48-52.

Multifunctional Hybrid Colloids: Organics and Inorganics Meet at the Nanoscale

Ana Torres-Suay[1], Sergio García[1], Maria Gascó[1], Pablo Martín[1], Juan F. Ferrer-Crespo[1], Francisco Pérez-Pla[1], Olaia Álvarez-Bermúdez[1,2], Katharina Landfester[2], Rafael Muñoz-Espí[1,*]

[1] *Institut de Ciència dels Materials (ICMUV), Universitat de València, Paterna, Spain*

[2] *Max Planck Institute for Polymer Research, Mainz, Germany*

*E-mail: rafael.munoz@uv.es

Colloidal methods, very especially those involving liquid–liquid heterophase systems, are very versatile for the preparation of polymer/inorganic hybrid nanoparticles and nanocapsules. On one hand, colloidal particles (both polymeric and inorganic) can act as a support for crystallization processes on their surface. On the other hand, the colloidal structures generated by micelles and surfactant-stabilized droplets serve as soft templates or nanoreactors for the controlled precipitation of inorganic materials [1, 2]. In this poster, we will provide an overview of the versatility of miniemulsion sytems for the synthesis of hybrid nanomaterials.

We present four topics under current investigation by our team. In all four cases, the confinement of chemical processes at the nanoscale of systems stays in the foreground.

(1) Magnetoresponsive catalytic nanoparticles comprised of polystyrene and metal oxides (CeO_2 and Fe_3O_4), applied in the catalytic hydration of amides. Pickering stabilization (i.e., the use of inorganic nanoparticles for the stabilization of emulsions) is used for the nanoparticle synthesis.

(2) Polymer/noble metal systems (with gold or palladium in metallic form) applied in the in the catalysis of the reduction of 4–nitrophenol and the Suzuki–Miyaura coupling reaction.

(3) Conducting hybrid nanoparticles of polyaniline or polypyrrole, incorporating CeO_2, applied in the formation of films.

(4) Confined crystallization of molybdenum and tungsten oxide catalysts within droplets, combining the miniemulsion technique with hydrothermal conditions.

[1] M. A. Hood, M. Mari, R. Muñoz-Espí. *Materials* **2014**, *7*, 4057–4087

[2] R. Muñoz-Espí, O. Álvarez-Bermúdez. In: D. J. McClements and S. M. Jafari (eds.). *Nanoemulsions: Formulation, Applications, and Characterization*, pp. 477–515. Academic Press-Elsevier, 2018.

Optical amplification in hollow-core negative-curvature fibers doped with perovskite $CsPbBr_3$ nanocrystals

Juan Navarro-Arenas[1,*], Isaac Suárez[1,2], Albert Ferrando[3], Andrés F. Gualdrón-Reyes[5], I. Mora-Seró[5], Juan Martínez-Pastor[1], Zhipei Sun[4]

[1)] Intituto de Ciencia de Materiales (ICMUV), Universidad de Valencia, C/ Catedrático José Beltrán, 2, E-46980 Paterna, Spain [2)] School of Telecommunications Engineering, Electronics Area, Camino del Molino s/n E 28942 Fuenlabrada, Spain [3)] Departament d'Òptica i Optometria i Ciències de la Visió, Universitat de València, Dr Moliner, 50, 46100 Burjassot, Valencia, Spain [4)] Department of Electronics and Nanoengineering, Aalto University, Tietotie 3, Otaniemi, 02150, Espoo, Finland [5)] Institute of Advanced Materials (INAM), Universitat Jaume I, Castelló 12006, Spain

*E-mail: juan.navarro-arenas@uv.es

In this paper [1] we intend to harness the potential performance of Hollow-Core Negative Curvature Fibers (HC-NCF) doped with $CsPbBr_3$ Perovskite Colloidal-NCs (PNPs), prepared by chemical synthesis, in the construction of all-fiber optical microdevices with gain properties. The colloidal solution can travel distances in the range of tens of centimetres while the NCs attach to the walls of the air gaps, as it shown in the photoluminescence (Pl) map of Fig. 1.b. The signals were deconvoluted by the sum of two Gaussian functions (solid lines in Fig. 1.a) in order to study the evolution of the Pl generated by the CW-laser pump (405 nm) and the probe signal light (515 nm) independently. Our optimized device achieved a gain figure of +3 dB under 405 mm continuous-wave pumping. This amplification can be described by means of a cascaded four-wave mixing third order non-linear effect (orange curve in Fig. 1.c). Also, the device's gain mechanism was accurately described by using an adopted model from the Erbium-doped fiber amplifiers theory (green curve, Fig. 1.c).

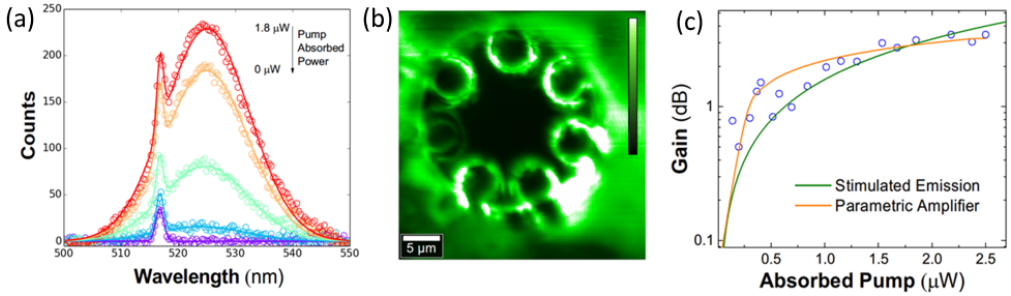

Figure 1: (a) Photoluminescence and signal laser as a function of increasing pump power of a PCF filled with a colloidal NCs. (b) Backscattered PL signal from a cross-section of the doped HC-NCF (c) Integrated power ratio of the output/input signal laser spectrum in dB units as a function of the absorbed pump power

[1] Navarro-Arenas, J.; Suárez, I.; Martínez-Pastor, J.P.; Ferrando, A.; Gualdrón-Reyes, A.F.; Mora-Seró, I.; Gao, S.-F.; Wang, Y.-Y.; Wang, P.; Sun, Z.; et al. *Optical Amplification in Hollow-Core Negative-Curvature Fibers Doped with Perovskite CsPbBr3 Nanocrystals*. Nanomaterials, **9**, 868 (2019).

METALLIC NANOSTRUCTURES OF METALLICA

Augusto Juste-Dolz[1], Miquel Avella-Oliver[1], Ángel Maquieira[1, 2]
[1]*Instituto Interuniversitario de Investigación de Reconocimiento Molecular y Desarrollo Tecnológico (IDM), Universitat Politècnica de València-Universitat de València, Camino de Vera s/n, E46022 Valencia, Spain*
aujusdol@upv.es
[2]*Departamento de Química, Universitat Politècnica de València, Camino de Vera s/n, E46022 Valencia, Spain*

The modification of inorganic surfaces with molecules patterned at nanoscale plays a key role in the scientific progress of nanotechnology and nanoscience [1]. In biosensing, nanostructured bioreceptors have proved to enhance the transduction of biointeractions, but the complexity, expensiveness, and low scalability of the standard nanofabrication techniques in the current state-of-the-art have hindered its development [2]. In recent years, microcontact printing (μCP) has emerged as an alternative tool to functionalize solid substrates with a periodic distribution of molecules in a simply and cost-effectiveness manner [3].

In this work, we present a novel and versatile approach to create nanostructured silver surfaces. It relies on patterning nanostructured bioreceptors on solid substrates by μCP and a biorecognition assay with antibodies labelled with gold nanoparticles. Gold nanoparticles act as nucleation centres and, a further Ag^+ incubation, develop nanostructured reliefs of metallic silver on the surface (Figure 1). Herein, we demonstrate the potential of this approach to fabricate reproducible and large-scale silver nanostructures of controllable thicknesses on different materials (glass, polycarbonate, and silicon).

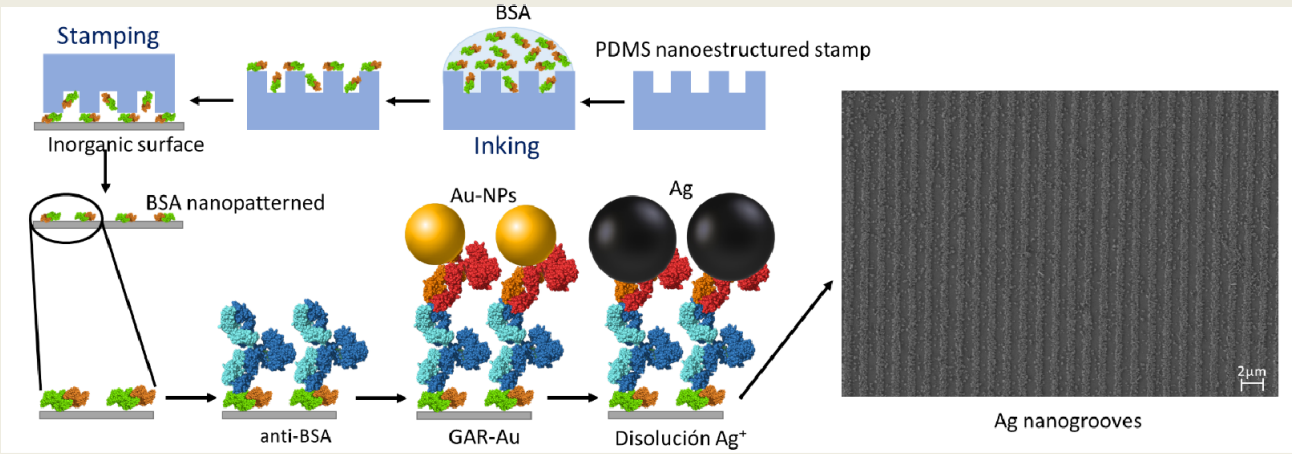

Figure 2. Bioreceptor micropatterning by microcontact printing and the subsequent silver precipitation.

This work was supported by MINECO (CTQ2016-75749-R), FEDER, GVA (PROMETEO II/2014/040) and PhD grant (UPV FPI 2017).

References

[1] Ravoo B.J. *J. Mater. Chem.* **2009**, 19, 8902-8906.

[2] Xing J. *J. Phys. D: Appl. Phys.* **2016**, 49, 29LT01.

[3] Avella-Oliver M., Carrascosa J., Puchades R. Maquieira A., *Anal. Chem.*, **2017**, 89, 9002-9008.

Porosity modulation in mesoporous solids through post-synthetic treatments

M. Dolores Garrido,[1] Carolina García-Llácer,[1] Pablo Piqueras,[1] Rahma Hanny,[1] Jamal El Haskouri,[1] José Vicente Ros-Lis,[2] Borja Díaz,[2] Francisco Pérez-Pla,[1] M. Dolores Marcos,[3] Aurelio Beltrán[1,2] and Pedro Amorós[1,2]

[1] *Institut de Ciència dels Materials (ICMUV), Universitat de València. P.O. Box 22085, 46071-Valencia, Spain*

[2] *Departament de Química Inorgànica, Universitat de València, C/ Dr. Moliner 50, Burjassot (València) Spain*

[3] *Centro de Reconocimiento Molecular y Desarrollo Tecnológico (IDM). Departamento de Química, Universitat Politècnica de València, Camino de Vera s/n, 46022, Valencia, Spain*

The original idea of the Mobil scientists to provide of ordered mesopores to amorphous silicas was based on the use of surfactant micelles as sacrificial templates. After silica condensation and template evolution, self-assembling between micelles and inorganic silica oligomers resulted in negative inorganic replicas of crystal-liquid mesophases. The space occupied by the micelles in the mesostructured solids generates mesopores by template elimination [1].

In this contribution, we present two chemical strategies allowing improving the porosity through nonselective or selective partial degradation/redissolution of the starting materials. We have tested these approaches using mesoporous Stöber and/or UVM-7 materials [2]. The non-selective treatment starts from mesoporous spherical Stöber particles synthesized through the atrane route. Once these particles have formed, and after the thermal extraction of the surfactant, the post-treatment to improve their porosity is carried out by suspending the material in a PBS medium and carefully adjusting the contact time and temperature. Interestingly, silica dissolution occurs in a homogeneous way throughout the whole mass of the particles without significant size reduction. Once a certain degradation is achieved, an additional thermal treatment is appropriate in order to increase stability and to avoid particle degradation progress. Large pore volumes and pore sizes can be achieved by this methodology. On the other hand, the selective degradation implies the previous incorporation of heteroelements (as isolates species, small oligomers or MO_x nanodomains) embedded in the silica walls. The atrane method shows a high efficacy with such aim, while allows that the heteroelement incorporation occurs in high proportions (when compared to other alternative protocols). We have introduced variable amounts of elements as Co and Zn inside the walls of UVM-7 and Stöber mesoporous particles. In the case of Co-UVM-7, the post-treatment in water/HCl medium favors the extraction of cobalt by forming Co-chloride complexes and leads to the formation of micropores. The final Co-free sample is a trimodal UVM-7 silica combining micro, meso and macropores. In the case of the Zn containing Stöber particles, we have used EDTA as a chelating agent. We have select a pH of compromise (pH ca. 4) to prevent significant degradation of the silica domains, but simultaneously allowing the existence of enough partially protonated EDTA ligands to extract Zn by selective complex formation. The changes in porosity have been monitored by XRD, TEM and N_2-adsorption-desorption measurements, and the elimination of the heteroelements (that also can be viewed as inorganic scarified template agents) has been controlled by mapping.

[1] C.T. Kresge et al. Nature **359**,710 (1992).

[2] J. El Haskouri et al. Inorg. Chem. **47**, 8267 (2008).

Chemical and mechanochemical preparative strategies to control the aggregation level in bimodal mesoporous nanoparticulated silicas

Valeriano Bellver,[1] Jamal El Haskouri,[1] José Vicente Ros-Lis,[2] Aurelio Beltrán[1,2] and Pedro Amorós[1,2]

[1] *Institut de Ciència dels Materials (ICMUV), Universitat de València. P.O. Box 22085, 46071-Valencia, Spain*

[2] *Departament de Química Inorgànica, Universitat de València, C/ Dr. Moliner 50, 46100 Burjassot (València) Spain*

Since the discovery in 1992 of the MCM-41 mesoporous materials, a large variety of related porous silicas have been described [1]. Among them, silicas combining pores structured at different length scales have attracted interest due to the favorable bidirectional mass diffusion (when compared to unimodal porous materials) [2]. In practice, these materials have been tested in a large variety of areas such as catalysis, remediation, sensing and medicine among others [2]. Depending on the specific application, aggregation or disaggregation conditions are preferred. Nonetheless, in all cases, it is desirable to achieve homogeneous grain size distributions. In particular, in the field of medicine, stable nanoparticles of maximum size around 150 nm are mandatory when intravenous administration is required. Despite the large number of publications dealing with the design of complex systems, the number of basic studies concerning to the aggregation of primary silica particles is scarce [3].

We have synthesized UVM-7 bimodal mesoporous silicas through the atrane method (developed in the ICMUV)[4]. The morphology of this silica-based family can be viewed as aggregates of primary mesoporous nanoparticles defining interparticle large pore systems. These primary particles are connected through siloxane bonds. We have used two mechanochemical strategies in order to achieve a reduction and homogenization of the size of the particle aggregates: ultrasounds irradiation and grinding in ball mill. In the first case, we have optimized the energy, the irradiation time and the pulse sequence. The objective is to provide the maximum energy to favor disaggregation but avoiding excessive energy that could be counterproductive because of stimulating the formation of interparticle Si-O-Si bonds by condensation of silanol moieties. In the second case, we have optimized jointly the grinding time and the size of the agate balls to obtain homogeneous grain sizes.

On the other hand, the chemical wet route we have developed is based on the addition of a second neutral surfactant in a very low proportion. The role of this last is to block the particle growth allowing to obtain truly colloidal suspensions (at least during two months). The particle isolation from these suspensions requires the use of ultracentrifugation (at least 45000 rpm).

In all three cases, the evolution of the as-synthesized UVM-7 silicas (during the corresponding post-treatment) has been monitored by DLS measurements. The nature of the final silicas has been studied through XRD, TEM and nitrogen adsorption-desorption measurements.

[1] C.T. Kresge et al. Nature **359**,710 (1992).

[2] X.-Y. Yang et al. Chem. Soc. Rev. **46**,481 (2017).

[3] R. R. Retamal Marín et al. Nanomaterials, **8**, 454 (2018)

[4] J. El Haskouri et al. Inorg. Chem. **47**, 8267 (2008).